

See discussions, stats, and author profiles for this publication at: <https://www.researchgate.net/publication/47728526>

# Iron Acyl Thiolato Carbonyls: Structural Models for the Active Site of the [Fe]-Hydrogenase (Hmd)

ARTICLE *in* JOURNAL OF THE AMERICAN CHEMICAL SOCIETY · NOVEMBER 2010

Impact Factor: 12.11 · DOI: 10.1021/ja1072228 · Source: PubMed

---

CITATIONS

41

---

READS

30

4 AUTHORS, INCLUDING:



[Marco Salomone-Stagni](#)

Libera Università di Bozen-Bolzano

18 PUBLICATIONS 586 CITATIONS

[SEE PROFILE](#)



[Wolfram Meyer-Klaucke](#)

Deutsches Elektronen-Synchrotron

193 PUBLICATIONS 5,297 CITATIONS

[SEE PROFILE](#)

Published in final edited form as:

*J Am Chem Soc.* 2010 December 1; 132(47): 16997–17003. doi:10.1021/ja1072228.

## Iron Acyl Thiolato Carbonyls: Structural Models for the Active Site of the [Fe]-Hydrogenase (Hmd)

**Aaron M. Royer,**

School of Chemical Sciences, University of Illinois at Urbana-Champaign, Urbana, IL 61801, USA

**Thomas B. Rauchfuss,**

School of Chemical Sciences, University of Illinois at Urbana-Champaign, Urbana, IL 61801, USA

**Marco Salomone-Stagni, and**

EMBL Outstation c/o DESY, Notkestraße 85, D-22603, Hamburg, Germany

**Wolfram Meyer-Klaucke**

EMBL Outstation c/o DESY, Notkestraße 85, D-22603, Hamburg, Germany

Thomas B. Rauchfuss: rauchfuz@uiuc.edu

### Abstract

Phosphine-modified thioester derivatives are shown to serve as efficient precursors to phosphine-stabilized ferrous acyl thiolato carbonyls via the reaction of phosphine thioesters and sources of Fe(0). The reaction generates both Fe(SPh)(Ph<sub>2</sub>PC<sub>6</sub>H<sub>4</sub>CO)(CO)<sub>3</sub> (**1**) and the *di*ferrous diacyl Fe<sub>2</sub>(SPh)<sub>2</sub>(CO)<sub>3</sub>(Ph<sub>2</sub>PC<sub>6</sub>H<sub>4</sub>CO)<sub>2</sub>, which carbonylates to give **1**. For the extremely bulky arylthioester Ph<sub>2</sub>PC<sub>6</sub>H<sub>4</sub>C(O)SC<sub>6</sub>H<sub>4</sub>-2,6-(2,4,6-trimethylphenyl)<sub>2</sub>, oxidative addition is arrested and the Fe(0) adduct of the phosphine is obtained. Complex **1** reacts with cyanide to give Et<sub>4</sub>N[Fe(SPh)(Ph<sub>2</sub>PC<sub>6</sub>H<sub>4</sub>CO)(CN)(CO)<sub>2</sub>] (Et<sub>4</sub>N[**2**]). <sup>13</sup>C and <sup>31</sup>P NMR spectra indicate that substitution is stereospecific and cis to P. The IR spectrum of [**2**]<sup>−</sup> in CH<sub>2</sub>Cl<sub>2</sub> solution very closely matches that for Hmd<sup>CN</sup>. XANES and EXAFS measurements also indicate close structural and electronic similarity of Et<sub>4</sub>N[**2**] to the active site of wild-type Hmd. Complex **1** also stereospecifically forms a derivative with TsCH<sub>2</sub>NC, but the adduct is more labile than Et<sub>4</sub>N[**2**]. Tricarbonyl **1** was found to reversibly protonate to give a thermally labile derivative, IR measurements of which indicate that the acyl and thiolate ligands are probably not protonated in Hmd.

### Introduction

The conversion of carbon dioxide to methane is accomplished on a massive scale biologically as indicated by world's natural gas reserves (6,254 trillion cubic feet).<sup>1</sup> The principal means by which microorganisms carry out this conversion has been delineated over the previous few decades.<sup>2</sup> This reduction is catalyzed by a sequence of enzyme-catalyzed steps that utilize several unusual cofactors. For example, the biochemical cycle starts with the conversion of CO<sub>2</sub> to a formamide using a methanofuran cofactor and ends with the hydrogenolysis of a CH<sub>3</sub>-S bond in coenzyme M. As a source on new ideas on catalysis, this collection of cofactors represent potentially rewarding targets. The biosynthesis and mode of action are areas ripe for discovery, and perhaps applications.

Correspondence to: Thomas B. Rauchfuss, rauchfuz@uiuc.edu; Wolfram Meyer-Klaucke.

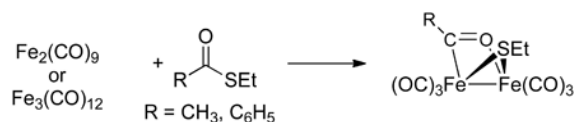
Supporting Information. Crystallographic analysis of **1**. Additional spectroscopic and preparative details (including protonation data). Reanalysis of EXAFS data for mHMD<sup>CN</sup> and mHMD<sup>CO</sup>.

The most recently elucidated step in the archaeal methanogenic cycle is the reduction of a stabilized carbocation to the corresponding methylene derivative.<sup>3</sup> Normally, this conversion is effected by a [NiFe]-hydrogenase in the hydrogenotrophic methanogens, but under conditions where nickel is insufficiently bioavailable, the organism up-regulates backup enzymes that catalyze the same conversion.<sup>4</sup> These enzymes are called H<sub>2</sub>-forming methylenetetrahydromethanopterin dehydrogenase (Hmd, PDB 3F47) and F<sub>420</sub>-dependent methylene tetrahydromethanopterin dehydrogenase (Mtd, PDB 3IQF). Hmd was originally thought to be free of metals because catalysis was found initially to be insensitive to the presence of CO. Later work showed that Hmd requires iron and is inhibited by CO.<sup>5</sup> Over the course of the preceding five years, the structure of the active site has been elucidated using both the native protein as well as mutants.<sup>6–10</sup> The protein harbors an active site consisting of the third example of a iron thiolato carbonyl center found in biology.<sup>11,12</sup> The fact that these species catalyze reactions involving H<sub>2</sub> is an example of convergent evolution and an indicator of the deep significance of the Fe-SR-CO system.<sup>11</sup>

The environment of the Fe center in Hmd is Fe(SR)(acyl)L(CO)<sub>2</sub>X, where L is an N-bonded ligand that is a derivative of either 2-hydroxypyridine or 2-pyridonate and X occupies an apparently labile site. In the crystal structure X has been modeled as oxygen (e.g. of water),<sup>7</sup> which is in line with the EXAFS analysis.<sup>13</sup> In the mutant protein, the oxygenic ligand is provided by an alcohol (Figure 1). Inhibited forms of the protein have been prepared where X is cyanide and CO. The cyanide derivative Hmd<sup>CN</sup> is stable, but its formation reverses at high dilution, whereas the CO-inhibited form Hmd<sup>CO</sup> is highly labile, in accord with the weak inhibiting effect of this ligand.<sup>3</sup> These inhibited forms, especially Hmd<sup>CO</sup> and Hmd<sup>CN</sup> represent suitable synthetic targets, since they are coordinatively saturated. Furthermore, models for Hmd<sup>CO</sup> could serve as precursors to catalytically active states.

From the structural perspective, the presence of the acyl ligand is striking. Fe-acyls are common in synthetic organometallic chemistry,<sup>14</sup> for example, (C<sub>5</sub>H<sub>5</sub>)(CO)<sub>2</sub>FeC(O)Me and [(CO)<sub>4</sub>FeC(O)Me]<sup>−</sup>, but are unusual in biology. Acyl nickel intermediates have been invoked in acetogenesis,<sup>15</sup> which is catalyzed by the enzyme acetyl Co-A synthase.<sup>16</sup> In Hmd, the acyl ligand may function as a trans directing group, stereoselectively labilizing the site that binds H<sub>2</sub>. Normally, acyl ligands are cis labilizing because of the facility of the η<sup>1</sup>- to η<sup>2</sup>-acyl conversion,<sup>17</sup> but if constrained in a chelate ring as in Hmd's active site, then we speculate that an acyl can exert a trans influence comparable to that of an aryl group.<sup>18</sup>

For first generation models of Hmd, we sought to incorporate the most distinctive ligand, the acyl. Prior to our work, acyl thiolato *monoiron* complexes were unknown, although *diiron* complexes of the type Fe<sub>2</sub>(SR)(acyl)(CO)<sub>6</sub> had been described. Specifically, Seyferth and coworkers prepared a series of diiron acyl thiolates via the formal oxidative addition of alkyl and arylthioesters to Fe(0) reagents (eq 1).<sup>19</sup>



(1)

The results presented in this paper suggest that these diiron compounds arise via monoiron acylthiolate complexes. The oxidative addition of thioesters has also been described for complexes of Rh(I)<sup>20</sup> and Pt(0)<sup>21</sup> and are of continuing interest for applications in organic synthesis.<sup>22,23</sup> Thioester-iron interactions may have been involved in the origin of life.<sup>24</sup>

We had previously described the oxidative addition of thioester-modified phosphines to Fe(0) reagents to give diiron  $\mu$ -thiolato species of the type  $\text{Fe}_2(\text{SPh})_2(\text{Ph}_2\text{PC}_6\text{H}_4\text{CO})_2(\text{CO})_3$ .<sup>25</sup> This diferrous species carbonylates to afford the metastable monomer *fac*-Fe(SPh)(Ph<sub>2</sub>PC<sub>6</sub>H<sub>4</sub>CO)(CO)<sub>3</sub> (**1**). This tricarbonyl was found to undergo monosubstitution to give derivatives mimicking other ligand-inhibited forms of Hmd, abbreviated Hmd<sup>L</sup>. In our preliminary report, we had not crystallized monomeric models of known inhibited states, but this problem has now been solved. Herein we describe the structural characterization of **1** and its cyanide derivative, which constitute close structural models for the active site of Hmd.

Following the discovery of the Fe-acyl bond in Hmd, several models have appeared. Hu and coworkers originally generated iron acyls stabilized by 2-mercaptopycoline derivatives.<sup>26</sup> More recently both the Hu and Pickett groups have developed acyl- or carbamoyl-pyridine derivatives of ferrous carbonyls.<sup>27</sup> The mechanism, including the role of the 2-pyridinol cofactor, has also attracted much interest from computational chemists.<sup>28</sup>

## Results

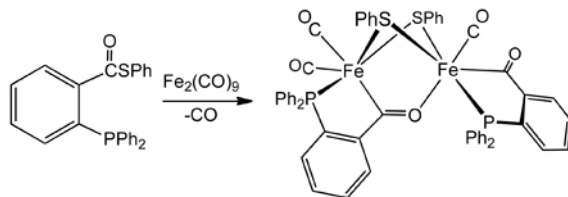
### Phosphine Thioesters

Thioester phosphines containing a variety of aryl and alkylthio substituents can be prepared via carbodiimide coupling. The new compounds are air-stable pale yellow to colorless crystalline solids. Such thioesters have been previously investigated as peptide coupling reagents ( $\text{Ph}_2\text{PC}_6\text{H}_4\text{C}(\text{O})\text{SEt}$ ).<sup>29</sup> Isomeric thioesters of the type  $\text{Ph}_2\text{PC}_6\text{H}_4\text{SC}(\text{O})\text{R}$  are also known (Scheme 1).<sup>30</sup>

### Fe(II)-Acyl Thiolates

We found that several of the phosphine thioesters afforded iron(II) acyl thiolato derivatives. A useful iron(0) source was  $\text{Fe}(\text{bda})(\text{CO})_3$  (bda = benzylideneacetone), but  $\text{Fe}_2(\text{CO})_9$  was also effective. Spectroscopic analysis of the reaction of  $\text{Ph}_2\text{PC}_6\text{H}_4\text{-2-C}(\text{O})\text{SPh}$  (**L<sup>a</sup>**) with the highly labile complex  $\text{Fe}(\text{CO})_3(\text{C}_8\text{H}_{14})_2$ <sup>31</sup> indicated displacement of only one coe ligand to give a monophosphine adduct. Thioesters derived from EtSH and *tert*-BuSH gave diiron compounds spectroscopically similar to the PhS derivative (see below), but these alkylthiolato compounds resisted carbonylation to the monoiron complexes (see below).

The simple thioester **L<sup>a</sup>** gave the cleanest and highest yielding reaction and became the main focus for our efforts. Treatment of a hot THF suspension of  $\text{Fe}_2(\text{CO})_9$  with **L<sup>a</sup>** was found to give diiron dithiolato complexes with the formula  $\text{Fe}_2(\text{SPh})_2(\text{CO})_3[\text{Ph}_2\text{PC}_6\text{H}_4\text{C}(\text{O})]_2$  (eq 2).<sup>25</sup>



(2)

This diiron species exists as a mixture of isomers that are proposed to differ with respect to the orientation of the  $\mu$ -SPh groups (Scheme 2).<sup>32</sup> Other aryl thioesters (Ar = C<sub>6</sub>H<sub>4</sub>-2-OMe, 2,4,6-*i*-Pr<sub>3</sub>C<sub>6</sub>H<sub>2</sub>) also gave derivatives of the type  $\text{Fe}_2(\text{SAr})_2(\text{Ph}_2\text{PC}_6\text{H}_4\text{CO})_2(\text{CO})_3$ , but these

conversions were less efficient. Using an extremely bulky arylthioester, we were able to arrest the oxidative addition. Thus, treatment of  $\text{Fe}_2(\text{CO})_9$  with  $\text{Ph}_2\text{PC}_6\text{H}_4\text{C}(\text{O})\text{SC}_6\text{H}_4$ -2,6-( $\text{Ar}^*$ )<sub>2</sub> ( $\text{Ar}^* = 2,4,6$ -trimethylphenyl) gave the monophosphine adduct of  $\text{Fe}(\text{CO})_4$ . The IR spectrum of this product matches that for known derivatives of the type  $\text{Fe}(\text{CO})_4(\text{PR}_3)$ .<sup>33</sup>

### Thioester Derivatives of Nitrogen-based Heterocycles

We also examined the reaction of thioester-functionalized *N*-heterocycles with  $\text{Fe}(\text{O})$  reagents (see Scheme 1). The thiophenolate esters of quinoline-8-carboxylic acid and 2-hydroxy-4-methyl-pyridine-6-acetic acid were synthesized by the usual coupling methods (Scheme 1). Both derivatives were reactive toward  $\text{Fe}_2(\text{CO})_9$  and  $(\text{bda})\text{Fe}(\text{CO})_3$ , but  $\text{Fe}_2(\text{SPh})_2(\text{CO})_6$  was the only Fe carbonyl product detected. Under the conditions (60 °C) necessary for reasonable conversions, the nitrogen heterocycles do not bind as robustly as the phosphine derivatives.

### $\text{Fe}(\text{SPh})(\text{Ph}_2\text{PC}_6\text{H}_4\text{CO})(\text{CO})_3$

Compound **1** was obtained by high pressure carbonylation of a warm solution of the aforementioned diiron derivative. Solutions of the monomer **1** were found to decarbonylate at room temperature, returning to the diiron complex, but solutions of **1** were stable for several minutes at  $<-10$  °C. Crystalline samples of **1** proved stable at room temperature in air for weeks. Exposure of a solution of complex **1** to 1 atm of  $^{13}\text{CO}$  at room temperature resulted in rapid ( $<5$  min.) exchange of all sites to give  $\text{Fe}(\text{SPh})(\text{Ph}_2\text{PC}_6\text{H}_4\text{CO})(^{13}\text{CO})_3$ . The  $^{31}\text{P}$  NMR spectrum of this species confirmed the arrangement of the CO ligands, since three separate  $^{13}\text{C}$ - $^{31}\text{P}$  couplings are observed with  $J = 58, 21$ , and  $16$  Hz. In  $\text{Fe}(\text{CO})_3(\text{PMe}_3)(\eta^2\text{-Me}_3\text{SiCCSiMe}_3)$ , the  $^{13}\text{CO}$ - $^{31}\text{P}$  coupling constants are 59 (trans) and 35 Hz (cis).<sup>34</sup>

### $[\text{Fe}(\text{SPh})(\text{Ph}_2\text{PC}_6\text{H}_4\text{CO})(\text{CN})(\text{CO})_2]^-$

Complex **1** reacts smoothly with cyanide to afford the anion  $[\text{Fe}(\text{SPh})(\text{Ph}_2\text{PC}_6\text{H}_4\text{CO})(\text{CN})(\text{CO})_2]^-$  (**[2]<sup>-</sup>**), isolated as its  $\text{Et}_4\text{N}^+$  salt. The  $^{13}\text{C}$  and  $^{31}\text{P}$  NMR spectra for  $\text{Et}_4\text{N}[\text{2}]$  and its  $^{13}\text{C}$ -labeled derivative indicate that substitution is stereospecific. The value of  $J(^{31}\text{P}, ^{13}\text{C})$  indicates that cyanide is located cis to the phosphine ligand.<sup>35</sup> Unlike **1**, solutions of **[2]<sup>-</sup>** are stable with respect to loss of CO as also seen for  $\text{Hmd}^{\text{CN}}$ .<sup>9</sup> The IR spectrum of **[2]<sup>-</sup>** in  $\text{CH}_2\text{Cl}_2$  solution also closely matches the cyanide-inhibited form of Hmd, wherein cyanation also proceeds stereoselectively<sup>9</sup> (Figure 2, Table 1).

The cyanide derivative was further characterized by X-ray absorption spectroscopy. The XANES spectrum, indicative of the electronic structure of the iron site, closely matches that of iron binding site in  $\text{mHmd}^{\text{CN}}$  in wild type.<sup>10</sup> The intense pre-edge peak for the new complex is resolved as a doublet, assigned tentatively to the  $1s\text{-}3d/4p$  transition(s).<sup>\*</sup> The XANES spectra for both the CN-inhibited enzyme as well as  $\text{Et}_4\text{N}[\text{2}]$  show a mild shoulder in their rising edge, followed by a sharp resonance at about 7130 eV and a broad resonance at about 7150 eV. The position of the subsequent minimum at 7170 eV is mainly attributed to the distance of those ligands dominating the EXAFS pattern. The high similarity of its position indicates strong similarities in the overall geometry of the active sites.

### Adducts with $\text{TsCH}_2\text{NC}$

Reminiscent of its reactivity toward cyanide, complex **1** was found to undergo substitution by  $\text{TsCH}_2\text{NC}$  under mild conditions.  $^{31}\text{P}$  NMR spectroscopic measurements show that

<sup>\*</sup>The high resolution in the *K*-edge region was achieved with the Si(220) monochromator with an intrinsic resolution of 0.4 eV vs 0.9 eV for Si(111).

substitution occurs in seconds at about  $-10\text{ }^{\circ}\text{C}$ . The formation of a single derivative ( $\delta_{70.7}$  vs  $\delta_{72.5}$  for **1**; see Table 1 for  $\nu_{\text{CO}}$  and  $\nu_{\text{CN}}$ ) indicates stereoselective substitution. The  $\text{TsCH}_2\text{NC}$ -substituted complex is stable in solution at temperatures below  $-10\text{ }^{\circ}\text{C}$ , but  $^{31}\text{P}$  NMR measurements indicate that over the course of several minutes at  $-5\text{ }^{\circ}\text{C}$ . The initial species converts to a mixture of three additional complexes, which are assumed to be isomers or the result of decarbonylation. At room temperature, this mixture simplifies over the course of a few minutes, as indicated by the appearance of two  $^{31}\text{P}$  NMR signals in a 1:1 ratio, assigned to metastable diiron derivatives of the type  $\text{Fe}_2(\text{SPh})_2(\text{Ph}_2\text{PC}_6\text{H}_4\text{CO})_2(\text{CO})(\text{RNC})_2$ .

## Protonation

Tricarbonyl **1** was found to undergo protonation at low temperatures to give unstable derivatives. In  $\text{CH}_2\text{Cl}_2$  solution at  $-30\text{ }^{\circ}\text{C}$ , protonation with  $\text{H}(\text{OEt})_2\text{BAr}^{\text{F}}_4(\text{Ar}^{\text{F}} = 3,5\text{-(CF}_3)_2\text{C}_6\text{H}_3)$  afforded a single product  $[\text{1H}]^+$  which lacks apparent hydride signals in its  $^1\text{H}$  NMR spectrum. The IR spectrum ( $-26\text{ }^{\circ}\text{C}$ ) showed  $\nu_{\text{CO}}$  bands ( $2090$ ,  $2041$ , and  $2024\text{ cm}^{-1}$ ), which are shifted by an average of  $18\text{ cm}^{-1}$  to higher energies vs those for **1**. Addition of  $\text{Et}_3\text{N}$  to this cold solution of  $[\text{1H}]^+$  cleanly returned **1** (IR analysis). The IR data are thus consistent with protonation at a ligand, probably the thiolate<sup>36</sup> or the acyl group.<sup>37</sup> The corresponding *S*- and *O*-protonation of the ferrous thiolate  $(\text{C}_5\text{H}_5)\text{Fe}(\text{CO})_2\text{SPh}$  and the ferrous acyl  $(\text{C}_5\text{H}_5)\text{Fe}(\text{CO})(\text{PPh}_3)\text{C}(\text{O})\text{Me}$ , respectively with  $\text{HBF}_4$  and  $\text{HBr}$  induces shifts in  $\nu_{\text{CO}}$  by  $40$  and  $32\text{ cm}^{-1}$ .<sup>36,37</sup> Upon warming its solution to  $20\text{ }^{\circ}\text{C}$ ,  $[\text{1H}]^+$  was found to convert to a new product, which decomposed over the course of a few minutes.

## Structure of $\text{Fe}(\text{SPh})(\text{Ph}_2\text{PC}_6\text{H}_4\text{CO})(\text{CO})_3$

The tricarbonyl monomer **1** was further characterized by X-ray crystallography (Figure 4).

The structure of **1** compares well with the recent structure of the C176A mutant of Hmd, which has been characterized at  $2.15\text{ \AA}$  resolution.<sup>7</sup> In this mutant, one cysteinyl ligand is replaced by one thiolate of dithiothreitol, which also provides an alcohol ligand in the coordination site trans to the acyl (see Figure 1).

## Conclusions

Thioester derivatives of 2-diphenylphosphinobenzoic acid are versatile multifunctional reagents that enable easy access to phosphine-stabilized metal acyl thiolato carbonyls. The PhS derivative was examined in detail and shown to adopt a structure very similar to the one modeled for the Fe site in Hmd<sup>CO</sup>.<sup>8</sup> The major difference is the presence of the phosphine ligand vs the pyridyl group of the GP cofactor, but the phosphorus center offers the distinct advantage of enabling  $^{31}\text{P}$  NMR analysis of reaction mixtures. The pathway for the oxidative addition of the thioester to  $\text{Fe}(0)$  is illuminated by the finding that an extremely bulky phosphine thioester gave an adduct of the type  $\text{Fe}(\text{Ph}_2\text{PC}_6\text{H}_4\text{COSR})(\text{CO})_4$ . The isolation of this adduct is consistent with phosphine coordination preceding the chelate-assisted oxidative addition<sup>38</sup> of the thioester group. The oxidative addition of the thioester can then be envisioned to proceed via coordination of the thioether-like sulfur center<sup>23</sup> (Scheme 3). In contrast, oxidative addition of simple thioesters to  $\text{Fe}(0)$  reagents proceeds in low yields to give  $[\text{Fe}(\text{I})]_2$  derivatives of the type  $\text{Fe}_2(\text{SR})_2(\text{CO})_6$  or  $\text{Fe}_2(\text{SR})(\text{C}(\text{O})\text{R}')(\text{CO})_6$ .<sup>19</sup>

Whereas the phosphine facilitates oxidative addition of the thioester, the low affinity of  $\text{Fe}(0)$  for pyridines<sup>39</sup> prevented incorporation of the more biomimetic *N*-heterocyclic ligand on the  $\text{Fe}(\text{CO})_3$  center. Reactivity studies reinforce the electronic similarity between our model and the active site. Hmd stereoselectively binds  $^{13}\text{CO}$  and  $\text{CN}^-$ .<sup>9</sup>  $^{31}\text{P}$  NMR data show



that **1** undergoes stereoselective substitution by both  $\text{CN}^-$  and  $\text{TsCH}_2\text{CN}$ , but CO is so labile in our model that stereoselective binding of  $^{13}\text{CO}$  was not observed (Scheme 4). The lability of the site trans to acyl combined with the bridging tendency of thiolate ligands explains the facile conversion of **1** into the related  $\text{Fe}_2(\text{SR})_2$  derivative.<sup>25</sup> Our results suggest that the Fe-GP cofactor might be expected to degrade via dimerization.

As indicated by comparisons of the XANES, EXAFS, and IR spectra for Hmd and  $\text{Hmd}^{\text{CN}}$  (*M. marburgensis*),  $[\text{Fe}(\text{SPh})(\text{Ph}_2\text{PC}_6\text{H}_4\text{CO})(\text{CN})(\text{CO})_2]^-$  replicates the major details of both the electronic and geometric structure of the active site. This close match provides compelling evidence for the presence of a ferrous center in Hmd. The oxidation state of the Fe center in Hmd has been of recurring interest,<sup>40</sup> but the issue should now be considered settled in light of this and related modeling work on acyl-containing models.<sup>26,27</sup>

The present results highlight the anomalous effect of cyanide on the IR spectrum of Hmd. In  $\text{Hmd}^{\text{CN}}$ , two  $\nu_{\text{CO}}$  bands are shifted to higher energies by 9 and 12  $\text{cm}^{-1}$ . In this conversion,  $\text{CN}^-$  is assumed to displace a labile ligand such as water. Nonetheless, it is extremely rare that  $\nu_{\text{CO}}$  bands shift to higher energy upon installing a cyanide ligand. For example the average of the two  $\nu_{\text{CO}}$  bands is 50  $\text{cm}^{-1}$  lower in  $[\text{Fe}(\text{SPh})(\text{Ph}_2\text{PC}_6\text{H}_4\text{CO})(\text{CN})(\text{CO})_2]^-$  than in  $\text{Fe}(\text{SPh})(\text{Ph}_2\text{PC}_6\text{H}_4\text{CO})(\text{CO})_3$ .<sup>9</sup> One possible explanation for this anomaly is that  $\text{CN}^-$  affects the second coordination sphere of the ferrous center in Hmd, such as the protonation state of the pyridone ligand.

Our tricarbonyl model was also susceptible to reversible protonation, but only with strong acids. The  $\nu_{\text{CO}}$  bands for the protonated tricarbonyl occur at 20–30  $\text{cm}^{-1}$  above those seen for  $\text{Hmd}^{\text{CO}}$ . Furthermore, the protonated derivative is unstable at temperatures above –30 °C.

## Experimental

### General Considerations

Unless otherwise indicated, reactions were conducted using standard Schlenk techniques ( $\text{N}_2$ ) at room temperature with stirring. All solvents were dried and degassed prior to use. Literature procedures afforded the following reagents: 2-diphenylphosphinobenzoic acid,<sup>41</sup> 2,6-dimesitylphenylthiol, 2,4,6-triisopropylthiol,<sup>42</sup> 2-hydroxy-4-methylpyridine-6-acetic acid,<sup>43</sup>  $[\text{H}(\text{Et}_2\text{O})]\text{BAr}^{\text{F}}_4$ ,<sup>44</sup> and  $\text{Fe}(\text{bda})(\text{CO})_3$ .<sup>45</sup> Benzenethiol, 2-methyl-2-propanethiol, ethanethiol,  $\text{TsCH}_2\text{NC}$ , and  $\text{Et}_4\text{NCN}$  were purchased from Sigma-Aldrich. DCC, 2-mercaptopyridine, and 4-dimethylaminopyridine were obtained from Fluka Analytical. EDAC (1-ethyl-3-(3-dimethylaminopropyl)carbodiimide hydrochloride) was purchased from Chem-Impex International.  $\text{MgSO}_4$  and  $\text{NaHCO}_3$  were purchased from Fisher Chemicals.  $\text{Fe}_2(\text{CO})_9$  was purchased from Strem Chemicals. Quinoline-8-carboxylic acid was purchased from Karl Industries. 2-Methoxythiophenol was obtained from SAFC Supply Solutions (St. Louis, MO).  $\text{K}^{13}\text{CN}$  was purchased from Isotec. The silica gel used was 230–400 mesh Siliaflash® P60 from Silicycle. Electrospray ionization-mass spectra (ESI-MS) were acquired using a Micromass Quattro QHQ quadrupole-hexapole-quadrupole instrument.  $^1\text{H}$  and  $^{31}\text{P}$  NMR spectra were acquired on Varian UNITY INOVA TM 500NB and UNITY 500 NB instruments. Elemental analyses were performed by the School of Chemical Sciences Microanalysis Laboratory utilizing a Model CE 440 CHN Analyzer. In situ IR spectroscopic measurements were obtained using a ReactIR 4000 (Mettler-Toledo) instrument.

The preparation and purification of thioesters was found to be slightly less cumbersome utilizing the water soluble reagent EDAC instead of DCC.

**Ph<sub>2</sub>PC<sub>6</sub>H<sub>4</sub>-2-C(O)SPh, L<sup>a</sup>**—To a stirred solution of PhSH (870 μL, 8.475 mmol) in CH<sub>2</sub>Cl<sub>2</sub> (20 mL) was added 2-diphenylphosphinobenzoic acid (2.36 g, 7.705 mmol) and DCC (1.75 g, 8.475 mmol). The reaction mixture was stirred 1 h, and the precipitated 1,3-dicyclohexylurea was filtered off. The yellow filtrate was concentrated under vacuum, and the residue was purified by column chromatography on silica gel, eluting with 50:1 hexane:ethylacetate. The light yellow fraction was evaporated to give a crystalline solid that was dried under vacuum. Yield: 2.5 g (82%). <sup>31</sup>P NMR (202 MHz, CD<sub>2</sub>Cl<sub>2</sub>): δ -5.53. FDMS m/z: 398.2 (Calcd for M<sup>+</sup>: 398.1). IR (CH<sub>2</sub>Cl<sub>2</sub>, cm<sup>-1</sup>): ν<sub>CO</sub> = 1677 (acyl). Anal. Calcd for C<sub>25</sub>H<sub>19</sub>OPS (found): C, 75.36 (75.08); H, 4.81 (4.82); N, 0.00 (0.51).

**Ph<sub>2</sub>PC<sub>6</sub>H<sub>4</sub>-2-C(O)SC<sub>6</sub>H<sub>3</sub>-2,6-(C<sub>6</sub>H<sub>2</sub>-2,4,6-Me<sub>3</sub>)<sub>2</sub>**—To a stirred solution of 2,6-dimesitylphenylthiol (1000 mg, 2.89 mmol) in CH<sub>2</sub>Cl<sub>2</sub> (20 mL) was added 2-diphenylphosphinobenzoic acid (884 mg, 2.89 mmol), 4-dimethylaminopyridine (35 mg, 0.29 mmol), and EDAC·HCl (830 mg, 4.33 mmol) successively. The reaction solution was stirred for 3.5 h, and then washed 3x with 1 N HCl (30 mL), followed by 2 x with saturated aqueous NaHCO<sub>3</sub> (30 mL), and once with water (30 mL). After drying over MgSO<sub>4</sub>, the solution was evaporated. The residue was extracted into hexanes (8 mL) and precipitated a white solid within 15 min. The solid was collected by filtration, washed with 5 mL of hexanes, and dried under vacuum. Yield: 1.32 g (74%). <sup>1</sup>H NMR (500 MHz, CD<sub>2</sub>Cl<sub>2</sub>): δ 1.96 (s, 12H, mesityl-2,6-CH<sub>3</sub>), 2.27 (s, 6H, mesityl-4-CH<sub>3</sub>), 6.86 (s, 5H, aryl-H), 6.98–7.35 (15 H, aryl-H), 7.54 (t, 1H, aryl-H). <sup>31</sup>P NMR (202 MHz, CD<sub>2</sub>Cl<sub>2</sub>): δ -8.39. ESI-MS m/z: 635.6 (Calcd for MH<sup>+</sup>: 635.3). IR (CH<sub>2</sub>Cl<sub>2</sub>, cm<sup>-1</sup>): ν<sub>CO</sub> = 1674 (acyl). Anal. Calcd for C<sub>43</sub>H<sub>39</sub>OPS (found): C, 81.36 (80.89); H, 6.19 (6.32); N, 0.00 (0.46).

**2-HO-4-Me-6-[CH<sub>2</sub>C(O)SPh]-C<sub>5</sub>H<sub>2</sub>N**—To a stirred solution of PhSH (61.4 μL, 0.5982 mmol) in THF (50 mL) was added 2-hydroxy-4-methylpyridine-6-acetic acid (100 mg, 0.5982 mmol) and DCC (123.4 mg, 0.5982 mmol) successively. The reaction mixture was stirred 4 days. Solvent was removed under vacuum, and CH<sub>2</sub>Cl<sub>2</sub> (20 mL) was added. The precipitated 1,3-dicyclohexylurea was filtered off. The filtrate was concentrated under vacuum, and the yellow residue was washed with hexanes. The solid was extracted into ~15 mL of EtOAc, and this extract was filtered through a ~5-cm. plug of silica gel. Solvent was removed by vacuum, and the residue was recrystallized from CH<sub>2</sub>Cl<sub>2</sub> by the addition of hexanes, giving a white powder. Yield: 62 mg (40%). <sup>1</sup>H NMR (500 MHz, CD<sub>2</sub>Cl<sub>2</sub>): δ 2.23 (s, 3H, 4-CH<sub>3</sub>), 3.89 (s, 2H, CH<sub>2</sub>C(O)S) 6.15 (s, 1H, pyridyl-H), 6.34 (s, 1H, pyridyl-H), 7.43 (m, 5H, SC<sub>6</sub>H<sub>5</sub>). ESI-MS m/z: 260.3 (Calcd for MH<sup>+</sup>: 260.1). IR (CH<sub>2</sub>Cl<sub>2</sub>, cm<sup>-1</sup>): ν<sub>CO</sub> = 1657 (acyl). Anal. Calcd for C<sub>14</sub>H<sub>13</sub>NO<sub>2</sub>S (found): C, 64.84 (64.96); H, 5.05 (5.61); N, 5.40 (6.14).

**Fe(Ph<sub>2</sub>PC<sub>6</sub>H<sub>4</sub>C(O)SC<sub>6</sub>H<sub>3</sub>-2,6-Ar\*<sub>2</sub>(CO)<sub>4</sub> (Ar\* = 2,4,6-trimethylphenyl)**—A solution of Ph<sub>2</sub>PC<sub>6</sub>H<sub>4</sub>C(O)SC<sub>6</sub>H<sub>3</sub>-2,6-Ar\*<sub>2</sub> (94.2 mg, 0.148 mmol) in 20 mL of CH<sub>2</sub>Cl<sub>2</sub> was transferred to a mixture 54 mg (0.148 mmol) of Fe<sub>2</sub>(CO)<sub>9</sub> in 10 mL of CH<sub>2</sub>Cl<sub>2</sub> at 0°C. The mixture was stirred for 15 min. and then allowed to warm to room temperature. The mixture was evaporated to dryness under vacuum, and the solid was rinsed with ~15 mL of hexanes. The solid was recrystallized from 15 mL Et<sub>2</sub>O/30 mL of hexanes. Yield: 90 mg (76 %). <sup>31</sup>P NMR (202 MHz, CD<sub>2</sub>Cl<sub>2</sub>): 872.0 (s). IR (THF, cm<sup>-1</sup>): ν<sub>CO</sub> = 2048, 1969, 1950, 1933. IR spectroscopic measurements indicated that a solution of the compound in refluxing THF remained unchanged for 24 h.

**Fe(SPh)(Ph<sub>2</sub>PC<sub>6</sub>H<sub>4</sub>CO)(CO)<sub>3</sub>, 1**—Under a stream of N<sub>2</sub>, a solution of Fe(bda)(CO)<sub>3</sub> (445 mg, 1.55 mmol) and Ph<sub>2</sub>PC<sub>6</sub>H<sub>4</sub>C(O)SPh (652 mg, 1.63 mmol) in 20 mL of benzene was heated to reflux for 4 h. The solution was evaporated under vacuum and washed with a few mL of Et<sub>2</sub>O. The brown crystalline solid was dried overnight to give 743 mg of diiron



dithiolato complexes. A solution of this mixture (985 mg, 0.992 mmol) in 6 mL of CH<sub>2</sub>Cl<sub>2</sub> was stirred under 1600 psi of CO at 60 °C for 24 h to give a near quantitative conversion to **1**. Pure samples of **1** could be obtained by slow crystallization at –30 °C (see below). For such carbonylations, the solution is first pressurized at 100–500 psi followed by careful venting. This gas-exchange procedure is repeated twice more. The bomb is then pressurized to 1400–1800 psi, with cooling of the bomb as needed to achieve the final pressure. <sup>31</sup>P NMR (202 MHz, CD<sub>2</sub>Cl<sub>2</sub>): δ 72.5. IR (CH<sub>2</sub>Cl<sub>2</sub>, cm<sup>–1</sup>): ν<sub>CO</sub> = 2075, 2025, 2001, 1629 (acyl). Single crystals of **1** suitable for X-ray diffraction were obtained by layering hexanes over a solution of 450 mg of **1** in 5 mL of CH<sub>2</sub>Cl<sub>2</sub> at –30 °C for 96 h. Orange crystals of **1** were manually separated from a brown unidentified powder.

**Fe(SPh)(Ph<sub>2</sub>PC<sub>6</sub>H<sub>4</sub>CO)(<sup>13</sup>CO)<sub>3</sub>, **1**<sup>13</sup>CO**—A solution of a mixture of **1** and **2** (8.5 mg, 0.009 mmol, ~9:1 in favor of **1**) in 1 mL of CH<sub>2</sub>Cl<sub>2</sub> in a J-Young NMR tube was frozen, and the tube was evacuated under vacuum. An atmosphere of 0.8 atm of <sup>13</sup>CO was introduced, and the tube was sealed. The solution was thawed and analyzed by <sup>31</sup>P NMR spectroscopy within 5 min. IR data were obtained within 25 min. <sup>31</sup>P NMR (202 MHz, CD<sub>2</sub>Cl<sub>2</sub>): δ 72.0 (d of d of d, <sup>2</sup>J<sub>CPtrans</sub> = 53, <sup>2</sup>J<sub>CPcis</sub> = 21, <sup>2</sup>J<sub>CPcis</sub> = 16 Hz). IR (CH<sub>2</sub>Cl<sub>2</sub>, cm<sup>–1</sup>): ν<sub>CO</sub> = 2027, 1980, 1957, 1629 (acyl).

**Et<sub>4</sub>N[Fe(SPh)(Ph<sub>2</sub>PC<sub>6</sub>H<sub>4</sub>CO)(CN)(CO)<sub>2</sub>], **3****—A solution of Et<sub>4</sub>NCN (51.6 mg, 0.330 mmol) in 5 mL of CH<sub>2</sub>Cl<sub>2</sub> was added to a solution of **1** (164 mg, 0.3304 mmol) in 20 mL of CH<sub>2</sub>Cl<sub>2</sub>. The solution was stirred 10 min. and then concentrated to 2 mL. An oil precipitated upon the addition of 10 mL of Et<sub>2</sub>O. The oil was dissolved in THF and reprecipitated by the addition of ether. The resulting oily solid was recrystallized from THF/Et<sub>2</sub>O twice more to give an orange tacky solid that converted to an orange powder upon vacuum drying. Yield: 115 mg (52%). <sup>31</sup>P NMR (202 MHz, CD<sub>2</sub>Cl<sub>2</sub>): δ 66.73 (s). ESI-MS (negative mode, m/z): 536.1 (Calcd for C<sub>28</sub>H<sub>19</sub>FeNO<sub>3</sub>PS: 536.0). IR (CH<sub>2</sub>Cl<sub>2</sub>, cm<sup>–1</sup>): ν<sub>CN/CO</sub> = 2094 (CN), 2013, 1954, 1597 (acyl). Anal. Calcd for C<sub>36</sub>H<sub>39</sub>FeN<sub>2</sub>O<sub>3</sub>PS. Found: C, 64.87 (64.14); H, 5.90 (5.99); N 4.20 (4.33).

**Et<sub>4</sub>N[Fe(SPh)(Ph<sub>2</sub>PC<sub>6</sub>H<sub>4</sub>CO)(<sup>13</sup>CN)(CO)<sub>2</sub>], **3**<sup>13</sup>CN**—A solution of Et<sub>4</sub>N<sup>13</sup>CN (17 mg, 0.108 mmol) was generated by K<sup>13</sup>CN and Et<sub>4</sub>NCl in MeOH followed by filtration to remove KCl. Solvent was removed by vacuum, and the residue was dissolved in 3 mL of CH<sub>2</sub>Cl<sub>2</sub> and added to a solution of **1** (54.0 mg, 0.108 mmol) in 5 mL of CH<sub>2</sub>Cl<sub>2</sub>. The solution was stirred 10 min. and evaporated under vacuum. Upon slurrying in Et<sub>2</sub>O, the product converted to an oily orange powder that was dried under vacuum. <sup>31</sup>P NMR (202 MHz, CD<sub>2</sub>Cl<sub>2</sub>): δ 66.7, doublet, <sup>2</sup>J<sub>CP</sub> = 24 Hz. IR (CH<sub>2</sub>Cl<sub>2</sub>, cm<sup>–1</sup>): ν<sub>CO</sub> = 2050, 2012, 1954, 1597 (acyl).

**Fe(SPh)(Ph<sub>2</sub>PC<sub>6</sub>H<sub>4</sub>CO)(CO)<sub>2</sub>(NCCH<sub>2</sub>Ts)**—A solution of **1** (99.6 mg, 0.185 mmol) in 3 mL of CH<sub>2</sub>Cl<sub>2</sub> was cooled to –30 °C. A background IR spectrum was recorded in situ. A solution of TsCH<sub>2</sub>NC (36.5 mg, 0.185 mmol) in 1 mL of CH<sub>2</sub>Cl<sub>2</sub> was added and IR spectra were collected every minute as the solution was allowed to warm. The CO region of the IR spectra changed cleanly between –10 to –6 °C over the course of ~30 min. <sup>31</sup>P NMR (202 MHz, CD<sub>2</sub>Cl<sub>2</sub>): δ 70.7 (s). IR (CH<sub>2</sub>Cl<sub>2</sub>, cm<sup>–1</sup>): ν<sub>CN/CO</sub> = 2153 (CN), 2038, 1983, 1615 (acyl). Upon warming the sample above –6 °C, three new <sup>31</sup>P NMR signals at 73.2, 72.6, and 72.2 were initially observed before many signals appeared at further times. Upon prolonged standing at room temperature, loss of CO was observed.

## Protonation of **1**

A solution of **1** (30 mg, 0.056 mmol) in 3 mL of CH<sub>2</sub>Cl<sub>2</sub> solution cooled to –72 °C was examined by Ft-IR spectroscopy to confirm its integrity. A was added with solution of

[H(Et<sub>2</sub>O)<sub>2</sub>]BAr<sup>F</sup><sub>4</sub> (56.4 mg, 0.056 mmol) in 1 mL of CH<sub>2</sub>Cl<sub>2</sub> stirring. Within 5 min. the IR spectrum confirmed complete conversion to a new product (IR: 2090, 2041, 2024 cm<sup>-1</sup>). Addition of Et<sub>3</sub>N (10 μL, 0.072 mmol, -72 °C), gave back **1**. The protonated product isomerizes slowly at -30 °C. Protonation was also conducted in a J.Young NMR tube by adding 15.3 mg (0.028 mmol) of **1** and 30.3 mg (0.028 mmol) [H(Et<sub>2</sub>O)<sub>2</sub>]BAr<sup>F</sup><sub>4</sub> followed by vacuum transfer of 0.8 mL of CD<sub>2</sub>Cl<sub>2</sub>. The Sample was warmed to -78 °C and inserted into the NMR probe that had been precooled to -50 °C. The sample was slowly warmed to -30 °C at which temperature the <sup>31</sup>P NMR signal for starting material disappeared and a new signal appeared at δ68.1. The spectrum remained unchanged over the course of 30 min. Upon allowing the sample to warm to 0 °C, no change was noted, but at 20 °C, we observed rapid growth of a new singlet in the <sup>31</sup>P NMR spectrum (δ76.7). After 5 min, the signal at δ68.1 had completely disappeared. At longer times at room temperature, many new <sup>31</sup>P NMR signals were observed. The resulting solution had an odor of thiol.

### XAS Data Collection

In a glove box, the powder sample (25 μL in volume) was transferred into plastic sample holders covered with polyimide windows, frozen in liquid nitrogen and kept at 4 K during the experiment. X-ray absorption spectra at the Fe Kedge were recorded in transmission mode at Wiggler station 7-3 (SSRL, Menlo Park, CA, USA) equipped with a Si(220) double crystal monochromator, a focusing mirror and a 30 element Ge solid-state fluorescence detector (Canberra). Energy axis of each scan was calibrated by a reference sample (Fe foil). Scan averaging was done with Athena,<sup>46</sup> normalization and data reduction were performed with the EXPROG<sup>47</sup> using  $E_0(\text{Fe}) = 7120 \text{ eV}$ .

### XAS Data Analysis

The extended X-ray absorption fine structure (EXAFS) oscillations were analyzed with EXCURV9.2,<sup>48</sup> and the  $\sigma^3$ -weighted spectra were used. Different integer coordination numbers were considered for the ligands CO, CN, C, O, N, P, and S. The fit index was used as a measure of the goodness of the fits. *Ab initio* theoretical phase and amplitude functions were generated within EXCURV. The experimental spectra are compared with the theoretical simulations based on small atom theory. No Fourier filtering was applied. The best model is described in Table 3 and the fit is shown in Figure 3.

### Supplementary Material

Refer to Web version on PubMed Central for supplementary material.

### Acknowledgments

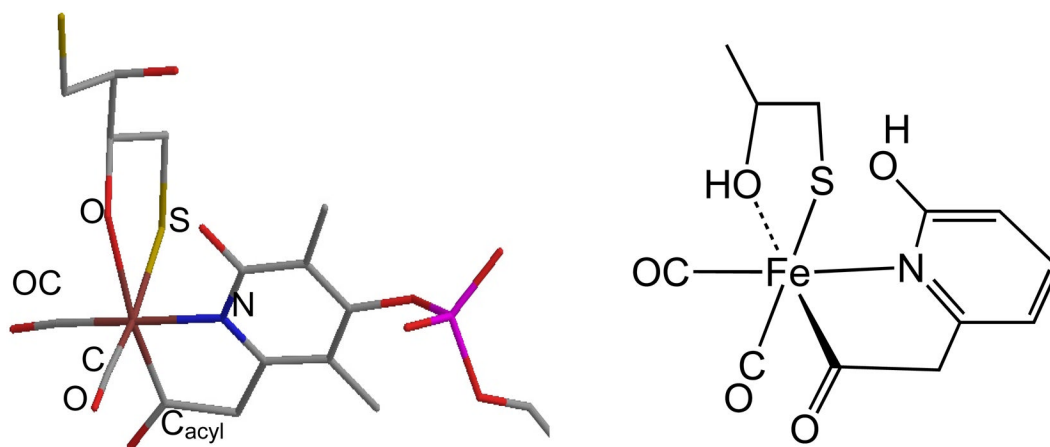
Research at Illinois was supported by the Department of Energy and the Petroleum Research Fund. We thank Dr. S. Shima (MPI-Marburg) for helpful advice. The authors are grateful to SSRL for providing beamtime and thank Erik Nelson and colleagues for their excellent support during the beamtime. Portions of this research were carried out at the Stanford Synchrotron Radiation Lightsource, a national user facility operated by Stanford University on behalf of the U.S. Department of Energy, Office of Basic Energy Sciences. The SSRL Structural Molecular Biology Program is supported by the Department of Energy, Office of Biological and Environmental Research, and by the National Institutes of Health, National Center for Research Resources, Biomedical Technology Program.

### References

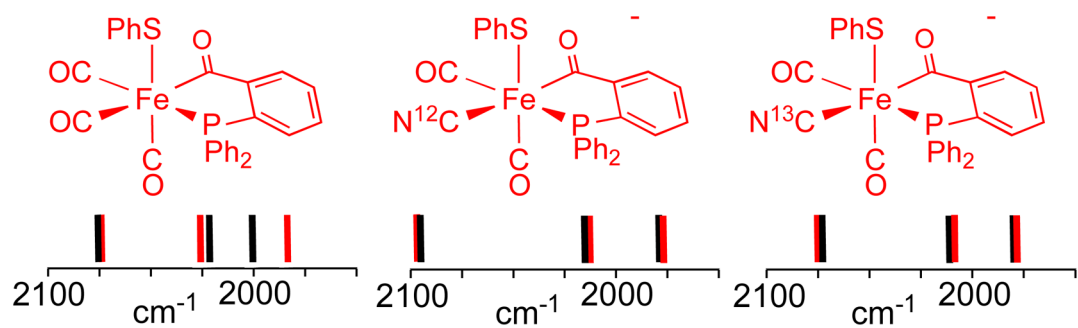
1. Energy Information Administration. World Proved Reserves of Oil and Natural Gas, Most Recent Estimates. Mar 3, 2009 <http://www.eia.doe.gov/emeu/international/reserves.html>
2. Thauer RK. Microbiology. 1998; 144:2377–2406. [PubMed: 9782487]
3. Shima S, Thauer RK. Chem Record. 2007; 7:37–46. [PubMed: 17304591]

4. Afting C, Hochheimer A, Thauer RK. Arch Microbiol. 1998; 169:206–210. [PubMed: 9477254]  
Afting C, Kremmer E, Brucker CAH, Thauer RK. Arch Microbiol. 2000; 174:225–232. [PubMed: 11081790]
5. Lyon EJ, Shima S, Buurman G, Chowdhuri S, Batschauer A, Steinbach K, Thauer RK. Eur J Biochem. 2004; 271:195–204. [PubMed: 14686932]
6. Shima S, Pilak O, Vogt S, Schick M, Stagni MS, Meyer-Klaucke W, Warkentin E, Thauer RK, Ermler U. Science. 2008; 321:572–575. [PubMed: 18653896]
7. Hiromoto T, Ataka K, Pilak O, Vogt S, Stagni MS, Meyer-Klaucke W, Warkentin E, Thauer RK, Shima S, Ermler U. FEBS Lett. 2009; 583:585–590. [PubMed: 19162018]
8. Hiromoto T, Warkentin E, Moll J, Ermler U, Shima S. Angew Chem Int Ed. 2009; 48:6457–6460.
9. Lyon EJ, Shima S, Boecher R, Thauer RK, Grevels FW, Bill E, Roseboom W, Albracht SPJ. J Am Chem Soc. 2004; 126:14239–14248. [PubMed: 15506791]
10. Korbas M, Vogt S, Meyer-Klaucke W, Bill E, Lyon EJ, Thauer RK, Shima S. J Biol Chem. 2006; 281:30804–30813. [PubMed: 16887798]
11. Armstrong FA, Fontecilla-Camps JC. Science. 2008; 321:498–499. [PubMed: 18653870]
12. Heinekey DM. J Organometal Chem. 2009; 694:2671–2680.
13. Salomone-Stagni M, Stellato F, Whaley CM, Vogt S, Morante S, Shima SBRT, Meyer-Klaucke W. Dalton Trans. 2010; 39:3057–3064. [PubMed: 20221540]
14. Plietker, B., editor. Iron Catalysis in Organic Chemistry. Wiley-VCH; Weinheim: 2008.
15. Tucci GC, Holm RH. J Am Chem Soc. 1995; 117:6489–6496.
16. Lindahl PA, Graham DE. Met Ions Life Sci. 2007; 2:357–415. Fontecilla-Camps JC, Amara P, Cavazza C, Nicolet Y, Volbeda A. Nature. 2009; 460:814–822. [PubMed: 19675641]
17. Ford PC, Rokicki A. Adv Organometal Chem. 1988; 28:139–206.
18. Hartwig, JF. Organotransition Metal Chemistry, from Bonding to Catalysis. University Science Books; New York: 2010.
19. Seyferth D, Womack GB, Archer CM, Dewan JC. Organometallics. 1989; 8:430–442.
20. Shaver A, Uhm HL, Singleton E, Liles DC. Inorg Chem. 1989; 28:847–851.
21. Minami Y, Kato T, Kuniyasu H, Terao J, Kambe N. Organometallics. 2006; 25:2949–2959.
22. Tokuyama H, Yokoshima S, Yamashita T, Lin SC, Li L, Fukuyama T. J Braz Chem Soc. 1998; 9:381–387. Fukuyama T, Lin SC, Li L. J Am Chem Soc. 1990; 112:7050–7051. Mori Y, Seki M. Org Synth. 2007; 84:285–294. Liebeskind LS, Srogl J. J Am Chem Soc. 2000; 122:11260–11261.
23. Looman SD, Giese S, Arif AM, Richmond TG. Polyhedron. 1996; 15:2809–2811.
24. Huber C, Wächtershäuser G. Science. 1997; 276:245–247. [PubMed: 9092471] Wächtershäuser G. Philos Trans Roy Soc. 2006; 361:1787–1806.
25. Royer AM, Rauchfuss TB, Gray DL. Organometallics. 2009; 28:3618–3620.
26. Chen D, Scopelliti R, Hu X. J Am Chem Soc. 2009; 132:928–929. [PubMed: 20041643]
27. Chen D, Scopelliti R, Hu X. Angew Chem Int Ed. 2010; 49:7512–7515. Turrell PJ, Wright JA, Peck JNT, Oganessian VS, Pickett CJ. Angew Chem Int Ed. 2010; 49:7508–7511.
28. Yang X, Hall MB. J Am Chem Soc. 2009; 131:10901–10908. [PubMed: 19722671] Dey A. J Am Chem Soc. 2010; 132:13892–13901. [PubMed: 20831194] Stiebritz MT, Reiher M. Inorg Chem. 2010; 49:5818–5823. [PubMed: 20527808]
29. Myers EL, Raines RT. Angew Chem, Int Ed. 2009; 48:2359–2363.
30. Zhang J, Wang H, Xian M. J Am Chem Soc. 2009; 131:3854–3855. [PubMed: 19256495]
31. Fleckner H, Grevels FW, Hess D. J Am Chem Soc. 1984; 106:2027–2032.
32. King RB. J Am Chem Soc. 1962; 84:2460.
33. Conder HL, Darensbourg MY. J Organomet Chem. 1974; 67:93–97.
34. Dennett JNL, Ferguson MJ, McDonald R, Takats J. Can J Chem. 2005; 83:862–868.
35. Rocchini E, Rigo P, Mezzetti A, Stephan T, Morris RH, Lough AJ, Forde CE, Fong TP, Drouin SD. J Chem Soc, Dalton Trans. 2000:3591–3602.
36. McGuire DG, Khan MA, Ashby MT. Inorg Chem. 2002; 41:2202–2208. [PubMed: 11952375]
37. Green MLH, Hurley CR. J Organomet Chem. 1967; 10:188–190.

38. Landvatter EF, Rauchfuss TB. *Organometallics*. 1982; 1:506.
39. Boxhoorn G, Cerfontain MB, Stufkens DJ, Oskam A. *J Chem Soc, Dalton Trans*. 1980:1336–1341.
40. Wang X, Li Z, Zeng X, Luo Q, Evans DJ, Pickett CJ, Liu X. *Chem Commun*. 2008:3555–3557. Guo Y, Wang H, Xiao Y, Vogt S, Thauer RK, Shima S, Volkers PI, Rauchfuss TB, Pelmenschikov V, Case DA, Alp EE, Sturhahn W, Yoda Y, Cramer SP. *Inorg Chem*. 2008; 47:3969–3977. [PubMed: 18407624]
41. Hoots JE, Rauchfuss TB, Wroblewski DA. *Inorg Syn*. 1982; 21:175.
42. Blower PJ, Bishop PT, Dilworth JR, Hsieh TC, Hutchinson J, Nicholson T, Zubieta J. *Inorg Chim Acta*. 1985; 101:63–65.
43. Royer AM, Rauchfuss TB, Wilson SR. *Inorg Chem*. 2008; 47:395–397. [PubMed: 18081276]
44. Brookhart M, Grant B, Volpe AF. *Organometallics*. 1992; 11:3920–3922.
45. Alcock NW, Richards CJ, Thomas SE. *Organometallics*. 1991; 10:231–238.
46. Ravel B, Newville M. *J Synchrotron Rad*. 2005; 12:537–541.
47. Nolting H-F, Hermes C. EXPROG: EMBL EXAFS data analysis and evaluation program package. 1992
48. Binsted N, Strange RW, Hasnain SS. *Biochemistry*. 1992; 31:12117–12125. [PubMed: 1280998]

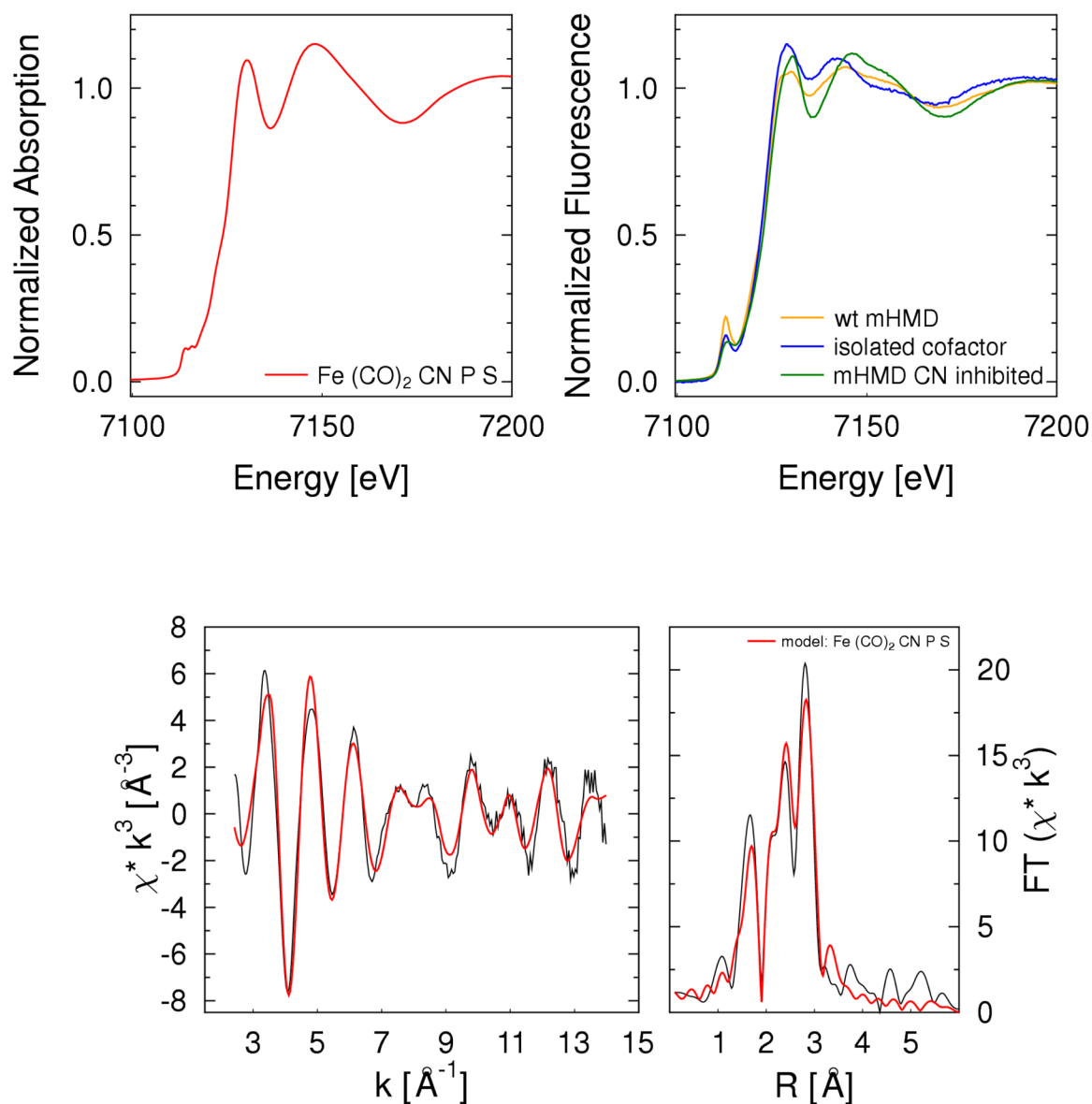


**Figure 1.** Stick models of the active site of the jHmd C176A mutant with dithiothreitol (DTT) replace cys176 (PDB 3H65) (*M. jannaschii*). One OH of the DTT occupies the site trans to acyl. Color scheme: brown, Fe; blue, N; red, O; purple, P; yellow, S; grey, C. See ref



**Figure 2.**  
IR spectral positions for  $\nu_{\text{CN}}$  and  $\nu_{\text{CO}}$  for selected model compounds and  $\text{Hmd}^{\text{CO}}$  and  $\text{Hmd}^{\text{CN}}$ .



**Figure 3.**

TOP: XANES spectrum of  $\text{Et}_4\text{N}[\text{Fe}(\text{SPh})(\text{Ph}_2\text{PC}_6\text{H}_4\text{CO})(\text{CN})(\text{CO})_2]$  (left) and wild-type Hmd from *M. marburgensis*, the isolated Fe-GP cofactor, as well as the cyanide-inhibited protein (right). BOTTOM: EXAFS spectrum and its Fourier transform with fits (red) for the model  $\text{Fe}(\text{CO})_3(\text{CN})\text{P}(\text{S})$  using the parameters in Table 2.

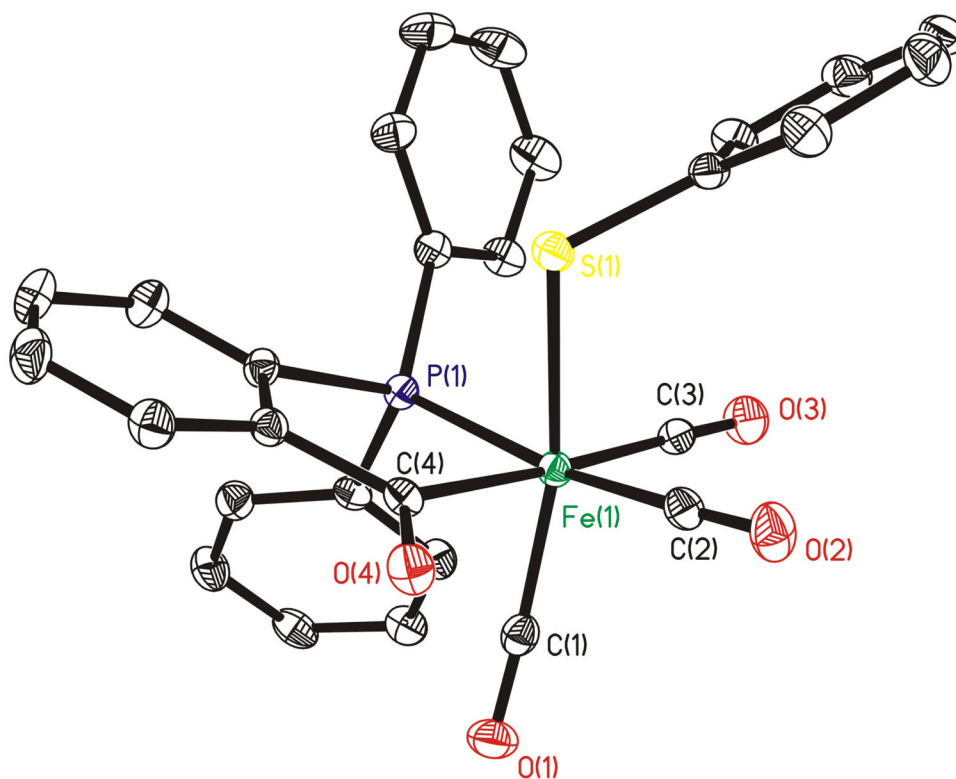
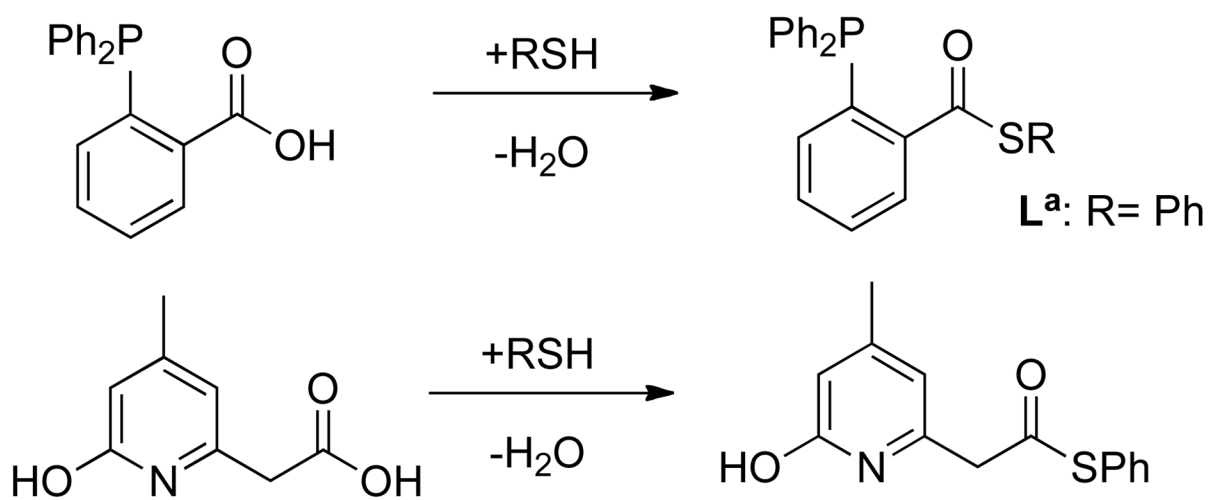
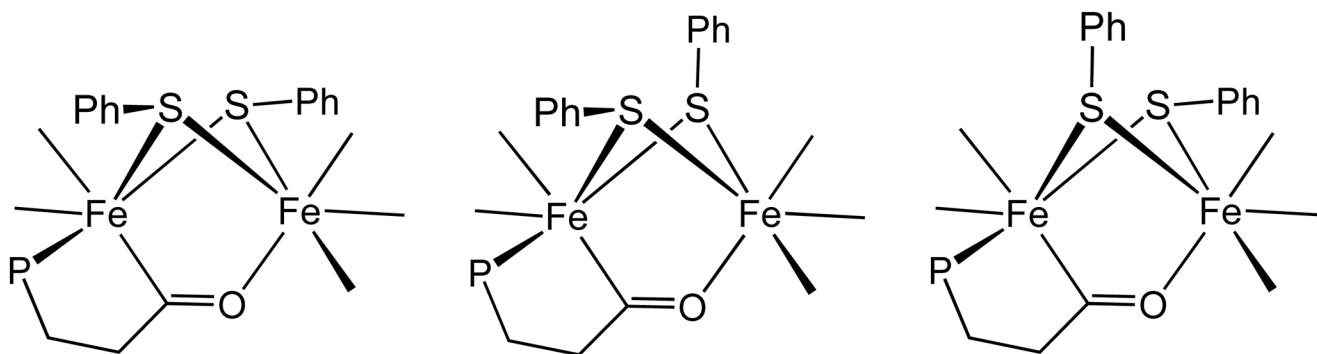


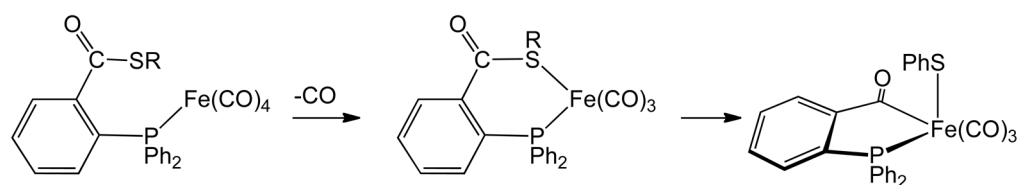
**Figure 4.**  
Structure of **1**, drawn with 35% probability ellipsoids. Hydrogen atoms were omitted for clarity.

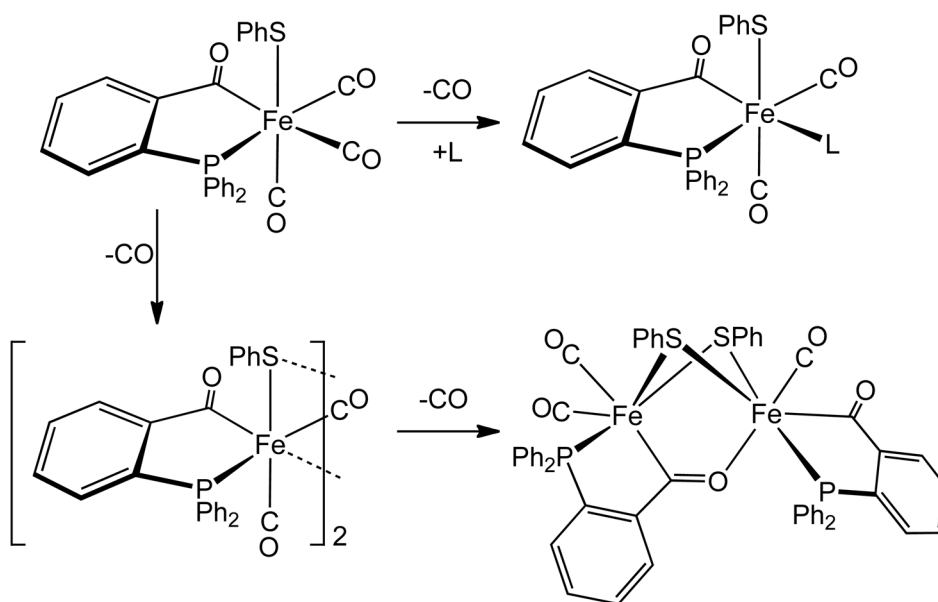


Scheme 1.



**Scheme 2.**  
Isomers proposed for  $\text{Fe}_2(\text{SPh})_2(\text{Ph}_2\text{PC}_6\text{H}_4\text{CO})_2(\text{CO})_3$ .

**Scheme 3.**



Scheme 4.



**Table 1**Selected IR Data for Model Compounds and for Hmd from *M. marburgensis*.<sup>9</sup>

Sample (models in CH <sub>2</sub> Cl <sub>2</sub> soln. unless otherwise indicated; enzyme in aqueous soln.)	$\nu_{\text{CO}}$ (cm <sup>-1</sup> )
Hmd <sup>CO</sup> from <i>M. marburgensis</i> <sup>9</sup>	2074, 2020, 1981
Fe(SPh)(Ph <sub>2</sub> PC <sub>6</sub> H <sub>4</sub> CO)(CO) <sub>3</sub> ( <b>1</b> ) (1:1 CH <sub>2</sub> Cl <sub>2</sub> :MeOH)	2075, 2025, 2001 (2077, 2028, 2005)
Hmd <sup>CN</sup> from <i>M. marburgensis</i> <sup>9</sup>	2090 ( $\nu_{\text{CN}}$ ), 2020, 1956
Et <sub>4</sub> N[Fe(SPh)(Ph <sub>2</sub> PC <sub>6</sub> H <sub>4</sub> CO)(CN)(CO) <sub>2</sub> ] (Et <sub>4</sub> N[ <b>2</b> ]) (1:1 CH <sub>2</sub> Cl <sub>2</sub> :MeOH)	2093 ( $\nu_{\text{CN}}$ ), 2013, 1954 (2093 (br, $\nu_{\text{CN}}$ ), 2026, 1973)
Et <sub>4</sub> N[Fe(SPh)(Ph <sub>2</sub> PC <sub>6</sub> H <sub>4</sub> CO)( <sup>13</sup> CN)(CO) <sub>2</sub> ] (Et <sub>4</sub> N[ <b>2</b> ] <sup>13</sup> CN)	2050 ( $\nu_{\text{CN}}$ ), 2012, 1954
Fe(SPh)(Ph <sub>2</sub> PC <sub>6</sub> H <sub>4</sub> CO)(CNCH <sub>2</sub> Ts)(CO) <sub>2</sub>	2154 ( $\nu_{\text{CN}}$ ), 2042, 1988

**Table 2**

Results of EXAFS Refinements for  $\text{Et}_4\text{N}[\text{Fe}(\text{SPh})(\text{Ph}_2\text{PC}_6\text{H}_4\text{CO})(\text{CN})(\text{CO})_2]$  (indices a, b, c and d indicate parameters that were refined jointly in order to lower the number of free parameters; Energy range 10 – 750 eV,  $EF = -6.3 \pm 0.3$  eV, Fit index: 0.954).

	ligand	<i>N</i>	<i>r</i> (Å)	$2\sigma^2$ (Å <sup>2</sup> )
2	CO	2	$1.81 \pm 0.01$	$0.016 \pm 0.003$
	CO	2	$2.93 \pm 0.01$	$0.012 \pm 0.002^a$
	CN	1	$2.07 \pm 0.03^c$	$0.012 \pm 0.004^b$
	CN	1	$3.19 \pm 0.03$	$0.012 \pm 0.002^a$
	C	1	$2.07 \pm 0.03^c$	$0.012 \pm 0.004^b$
	S	1	$2.32 \pm 0.02$	$0.008 \pm 0.004$
	P	1	$2.18 \pm 0.06$	$0.02 \pm 0.01$

**Table 3**Selected Bond Lengths (Å) for **1** and mHmd<sup>CO</sup>.

bond	compound 1	Hmd <sup>CO</sup> <i>M. jannaschii</i>
Fe1 - CO1	1.7844 (0.0018)	1.8260 (0.0081)
Fe1 - CO2	1.8229 (0.0019)	1.8260 (0.0081)
Fe1 - CO3	1.8395 (0.0018)	1.8260 (0.0081)
Fe1 - C <sub>acyl</sub> <sup>4</sup>	2.0202 (0.0016)	1.927 (0.044)
Fe1 - N	-	2.0194 (0.076)
Fe1 - S1	2.3457 (0.0005)	2.3162 (0.0056)

**Table 4**Selected Bond Lengths (Å) for **2** and mHmd<sup>CN</sup>.

bond	compound <b>2</b>	Hmd <sup>CN</sup> <i>M. jannaschii</i>
Fe1 - CO1	1.81 ± 0.01	1.776 ± 0.006
Fe1 - CO2	1.81 ± 0.01	1.776 ± 0.006
Fe1 - CN3	2.07 ± 0.03	2.06 ± 0.01
Fe1 - C <sub>acyl</sub> 4	2.07 ± 0.03	1.89 ± 0.01
Fe1 - N	-	1.97 ± 0.01
Fe1 - S1	2.32 ± 0.02	2.342 ± 0.006
Fe1 - P1	2.18 ± 0.06	-